2006

ZnO-nanoparticle-coated carbon nanotubes demonstrating enhanced electron field-emission properties

Joshua M. Green

lifeng Dong

Timothy Gutu

jun Jiao

J F. Conley Jr.

See next page for additional authors

Recommended Citation

Green, Joshua M., Lifeng Dong, Timothy Gutu, Jun Jiao, John F. Conley Jr, and Yoshi Ono. "ZnO-nanoparticle-coated carbon nanotubes demonstrating enhanced electron field-emission properties." Journal of Applied Physics 99, no. 9 (2006): 094308.

Enhanced field emission from cerium hexaboride coated multiwalled carbon nanotube composite films: A potential material for next generation electron sources

Rajkumar Patra,[1] S. Ghosh,[1,a)] E. Sheremet,[2] M. Jha,[3] R. D. Rodriguez,[2] D. Lehmann,[2] A. K. Ganguli,[3] O. D. Gordan,[2] H. Schmidt,[4] S. Schulze,[5] D. R. T. Zahn,[2] and O. G. Schmidt[4,6]

[1]*Nanostech Laboratory, Department of Physics, Indian Institute of Technology Delhi, New Delhi-16, India*
[2]*Semiconductor Physics, Technische Universität Chemnitz, 09126 Chemnitz, Germany*
[3]*Department of Chemistry, Indian Institute of Technology Delhi, New Delhi-16, India*
[4]*Material Systems for Nanoelectronics, Technische Universität Chemnitz, 09126 Chemnitz, Germany*
[5]*Solid Surfaces Analysis, Technische Universität Chemnitz, 09126 Chemnitz, Germany*
[6]*Institute for Integrative Nanosciences, IFW Dresden, Helmholtzstrasse 20, 01069 Dresden, Germany*

(Received 4 January 2014; accepted 13 February 2014; published online 4 March 2014)

Intensified field emission (FE) current from temporally stable cerium hexaboride (CeB_6) coated carbon nanotubes (CNTs) on Si substrate is reported aiming to propose the new composite material as a potential candidate for future generation electron sources. The film was synthesized by a combination of chemical and physical deposition processes. A remarkable increase in maximum current density, field enhancement factor, and a reduction in turn-on field and threshold field with comparable temporal current stability are observed in CeB_6-coated CNT film when compared to pristine CeB_6 film. The elemental composition and surface morphology of the films, as examined by scanning electron microscopy, transmission electron microscopy, and energy dispersive X-ray measurements, show decoration of CeB_6 nanoparticles on top and walls of CNTs. Chemical functionalization of CNTs by the incorporation of CeB_6 nanoparticles is evident by a remarkable increase in intensity of the 2D band in Raman spectrum of coated films as compared to pristine CeB_6 films. The enhanced FE properties of the CeB_6 coated CNT films are correlated to the microstructure of the films. © *2014 AIP Publishing LLC*. [http://dx.doi.org/10.1063/1.4866990]

I. INTRODUCTION

Field electron emission (FE) from various nanostructured materials is a promising research area, because of its potential applications in electron microscopes, field emission displays, microwave devices, X-ray sources, etc. FE is a quantum mechanical process where electrons near the Fermi level can tunnel through an energy barrier and escape to the vacuum level upon application of a high electric field.[1,2] With the advancement of research in growth and synthesis of carbon nanotubes (CNTs) the importance of FE has significantly enhanced in both fundamental physics and technology.[3] For high spatial, temporal, and energy resolutions, present day transmission electron microscopes (TEM) and scanning electron microscopes (SEM) require a point electron source that ensures high brightness and good temporal coherence. A cold field emitter (CFE) offers the highest brightness and temporal coherence over other types of electron sources, such as the Schottky emitter and the thermionic emitter. Because of their high melting point, mechanical strength, chemical stability, low work function, and stable specific resistance,[4,5] rare earth hexaborides like lanthanum hexaboride (LaB_6) and cerium hexaboride (CeB_6) were identified as the most promising electron source materials[6–11] for many small spot size applications such as surface analysis and metrology as well as high current applications such as microwave tubes, electron beam lithography, electron beam welders, X-ray sources, and free electron lasers. In addition, rare earth hexaborides can work at low operational temperature and have a long service life when used as a cathode material. For CFE sources, the brightness is associated with the emission current density (J), which can be described by the Fowler-Nordheim (FN) Eq. (1), as given below

$$J = \frac{a\beta^2 E^2}{\varphi}\exp\left(-\frac{b\varphi^{3/2}}{\beta E}\right), \tag{1}$$

where $a = e^3/8\pi h_P = 1.54434 \times 10^{-6}\,\mathrm{A\,eV\,V^{-2}}$ and $b = \frac{8\pi}{3}\cdot\frac{(2m_e)^{1/2}}{eh_P} = 6.83089 \times 10^9\,\mathrm{eV^{-3/2}\,V\,m^{-1}}$, E is the applied field strength (in V/μm), φ is the work function of the emitting material, and β is the field enhancement factor. Geometrically, this factor is defined as $\beta = h/r$, where h is the height and r is the radius of curvature of the emitting center. Therefore, the morphology of the emitter surface plays an important role in FE enhancement. Apart from the β factor, the turn-on field, the maximum current density, and the stability of FE current also determine the quality of a field emitter.

Recently, it has been reported that a turn-on electric field of ~ 7.6 V/μm with a field enhancement factor of $\sim$320 can be achieved in single crystalline CeB_6 nanowires.[5] In our recent work[12] further improvement in field enhancement

a)Author to whom correspondence should be addressed. Electronic mail: santanu1@physics.iitd.ac.in

factor with the same turn-on field was demonstrated for CeB_6 nanorods. However, for making an efficient CFE source, further reduction in turn-on field and enhancement of current stability, retaining a large β value are important. Particularly, temporal stability of field emission current is a crucial issue before using this material for any practical application. The inherent current fluctuation from pristine CNT can be reduced by coating CeB_6 nanoparticles on CNT.

This work is motivated to portray CeB_6 coated CNT film as prospective replacement of hexaboride filament for future electron source in electron microscopes. FE properties of CNT and CeB_6 can independently be found in the literature though, to the best of our knowledge, there is no report so far on composite of CeB_6 with CNT as FE source. An attempt has been made to correlate the FE results with the microstructure of the films by Raman spectroscopy and electron microscopy.

II. EXPERIMENTAL

A. Sample preparation

Multiwalled CNT (MWCNT) film was grown on iron coated p-Si (100) substrate by microwave plasma enhanced chemical vapor deposition (MPECVD) technique, as described in our previous reports.[13,14] 0.05 g of the as-obtained pure polycrystalline CeB_6, dispersed in 2.0 ml of ethanol: ethylene glycol mixture (1:1 volume ratio), was deposited on the MWCNT films by spin coating at 3000 rpm for 60 s followed by a slow drying process (200 °C at the rate of 20 °C/h). The process of CeB_6 spin coating was repeated twice. The film was further dried in Ar atmosphere at 200 °C for 6 h with slow heating and cooling rates (20 °C/min). The synthesis of CeB_6 was carried out by a low temperature borothermal reduction using a cerium precursor (cerium oxalate) (synthesized by reverse micellar route where cetyl trimethyl ammonium bromide (CTAB) was used as surfactant) and boron as the starting materials. The borothermal reduction of the cerium precursors was performed at 1300 °C in an inert (argon) atmosphere following a similar procedure reported previously.[12]

B. Characterization

Field emission scanning electron microscopy (FESEM) (FEI, Quanta 3D FEG, operated at 10 kV) and energy dispersive X-ray (EDX) analysis (Manufacturer: FEI, Model: Nano SEM 200, operated at 5 kV) were used to examine the morphology and composition. TEM (Philips, CM 20 FFG) with 200 kV electron beam was performed to examine the microstructure. Micro-Raman spectroscopy was performed using a single stage monochromator (Horiba JY, LabRam HR800) and a laser excitation of $\lambda = 514.5$ nm with a laser power below 1.0 mW in order to reduce sample heating. The laser beam was focused onto the sample surface with a 100× objective (N.A. = 0.9).

The FE properties were investigated using a very high vacuum (VHV) compatible FE set up in diode geometry. The distance between the anode (a stainless steel plate) and the cathode was kept constant at 200 μm. The electric field was varied from 1.75 to 15.0 V/μm at constant pressure of 7.5×10^{-7} Torr. Direct current (DC) voltage and current were measured using a high voltage DC power supply (Stanford Power Supply, PS 350) and an amperemeter (Keithley, 2000 Multimeter). Furthermore, the FE stability of the samples was checked for 7 h by monitoring the fluctuations of the current density at a sampling interval of 10 s at a constant electric field of 12.0 V/μm.

III. RESULT AND DISCUSSION

FESEM (Figure 1(a)) and TEM (Figure 1(b)) images of the film revealed the growth of CeB_6 nanoparticles (i) at the tips and sides of CNT walls and (ii) on the Si substrate.

In situ EDX (Figure 2(a)) with SEM, employed for elemental identification, confirmed the presence of boron, cerium, carbon along with iron (as catalyst), oxygen, silicon (as substrate). The signature of Al came from the SEM sample holder. The quantity of coated material was too small to get an intense line for Ce and B like other elements as indicated in Figure 2(a). However, existence of Ce and B along with C were clearly seen by SEM-EDX element mapping (Figures 2(b)–2(e)).

Raman spectroscopy is the method of choice to analyze carbon nanomaterials in electronic devices and to evidence modifications due to the CNT interaction with its environment such as metallic contacts.[15] Here, we aim at the impact of CeB_6 nanoparticles on the vibrational and electronic properties of CNT. Comparative normalized Raman spectra of pristine CNT and CeB_6-coated CNT samples are shown in Figure 3 (normalized with respect to the G band).

Both spectra revealed the typical signature of graphitic and disordered-induced vibrational modes[16] of carbon nanomaterials with sp^2 hybridization. The most prominent features in the spectral region from 1200 to 2800 cm^{-1} correspond to the D, G, and 2D (G′) bands, around 1350 cm^{-1}, 1578 cm^{-1}, and 2700 cm^{-1}, respectively.[17] Contrary to the D band, the 2D band, involving the creation of an electron and a hole near the K point and their recombination mediated by the inelastic scattering by two phonons, does not require the presence of defects on sp^2 carbon in order to be active (momentum is conserved by the creation of two phonons with opposite wavevectors).[18] The Raman bands in Figure 3 were fitted with Lorentzian functions; the parameters deduced from the fitting are shown in Table I. Other two-phonon features with lower intensity were

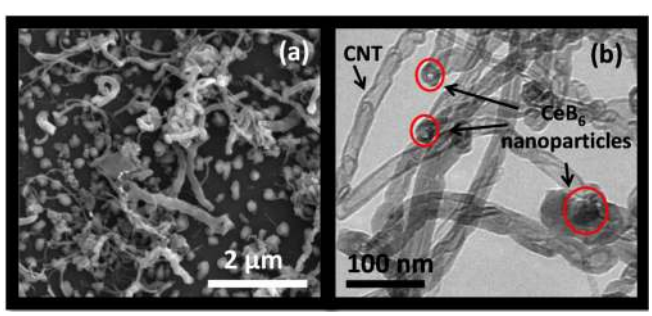

FIG. 1. (a) FESEM images of CeB_6-coated CNT film (b) TEM image of CeB_6-coated CNT film where the CeB_6 nanoparticles on CNT walls are marked by arrows.

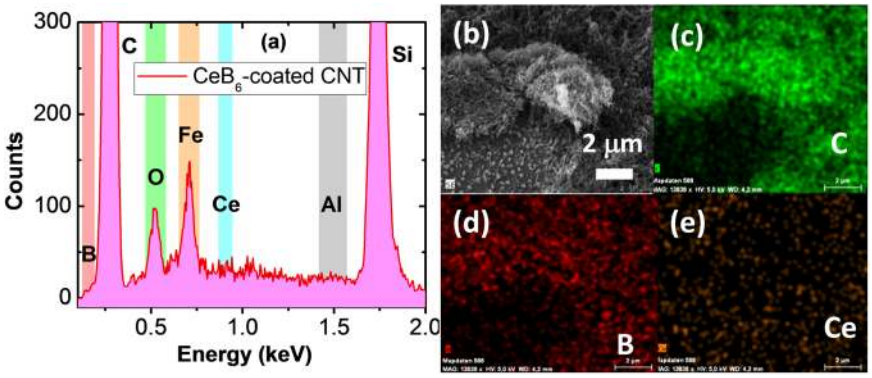

FIG. 2. EDX spectra of (a) CeB_6-coated CNT film indicating the presence of C, O, Fe, Al, Si, B, and Ce. (b-e) SEM and EDX mapping of CeB_6-coated CNT showing presence of C, Ce and B.

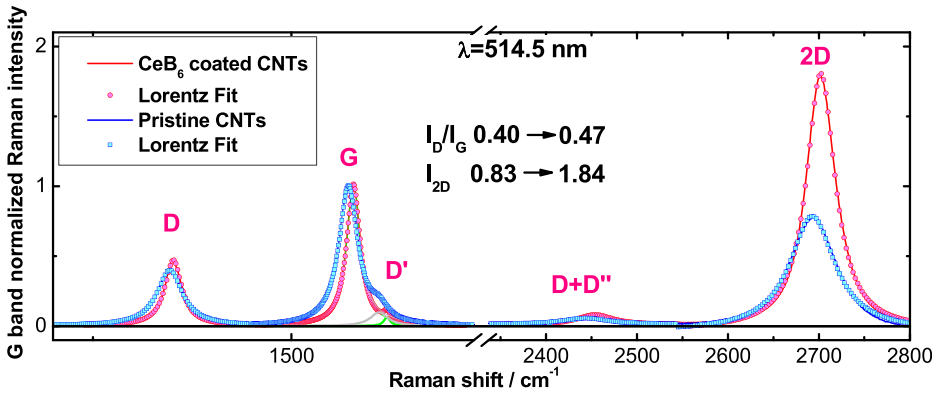

FIG. 3. Raman spectra of pristine (blue) and CeB_6-coated (red) CNTs under green laser excitation ($\lambda = 514.5$ nm) normalized to the G band of the CNTs. Each peak was individually fitted using a Lorentzian peak.

also observed around 1620 cm^{-1} and 2450 cm^{-1} corresponding to the defect-induced D′ and D + D″ bands, respectively. The most remarkable effect of CeB_6 on the Raman spectra of CNT is the pronounced enhancement of the 2D band. In addition, a decrease of the full width at half maximum (FWHM) of all peaks and a blue shift in their positions are observed.

There are two possible explanations for the spectral changes observed in the Raman spectra. The 2D band in graphene is highly sensitive to external perturbations and to changes in the electronic structure caused by defects, electric field, and doping.[17] However, there are very few reports on the intensity change of the 2D band in CNTs. Due to dielectric screening, it was predicted that any material covering the CNT will modify the exciton transition energies and equivalently, the electronic structure of single walled nanotubes (SWNTs) as a function of dielectric constant of the covering material.[19] The effect of surrounding material on the transition energies was experimentally confirmed by photoluminescence (PL) results of SWCNTs immersed in organic solvents with dielectric constants up to 37,[20] and SWCNTs non-covalently functionalized by porphyrins.[21,22] On the other hand, it was proposed that doping and charge transfer may play the main role in the changes of electronic structure of SWCNTs. According to Safar *et al.*[23] the G band position is indicative of charge transfer but the intensity of the 2D band in SWCNTs is more sensitive to the slope of the electronic energy dispersion than the G band. In other words, the 2D band enhancement can occur due to the changes in electronic structure of CNTs, which can be caused either by dielectric screening due to the surrounding material (in this case CeB_6, with dielectric constant about 8.4 at 2.4 eV,[24]) or by the charge transfer that modifies the electronic transition energies. Although a detailed theoretical study is still needed to achieve a comprehensive understanding of the phonon

TABLE I. Parameters of the Raman peaks deduced from Lorentzian fits. The error values have been deduced from the fitting. The parameters obtained for the pristine CNT sample are shown in black letters while those for the CeB_6-coated CNT sample are shown in bold letters.

Pristine CNT **CeB_6-coated CNT**	D	G	D′	D + D″	2D
FWHM (cm^{-1})	38.7 ± 0.10	28.88 ± 0.08	26.8 ± 0.8	61.0 ± 2.0	60.4 ± 0.5
	25.6 ± 0.01	**20.7 ± 0.10**	**10.0 ± 1.0**	**49.0 ± 3.0**	**38.4 ± 0.2**
Position (cm^{-1})	1346.9 ± 0.03	1571.86 ± 0.02	1610.4 ± 0.2	2443.5 ± 0.4	2692.8 ± 0.10
	1351.5 ± 0.01	**1578.23 ± 0.03**	**1620.4 ± 0.3**	**2454.0 ± 0.7**	**2702.11 ± 0.04**
Area	24.3 ± 0.10	45.1 ± 0.1	4.1 ± 0.1	4.3 ± 0.2	78.3 ± 0.7
	18.9 ± 0.01	**32.9 ± 0.1**	**0.9 ± 0.1**	**5.6 ± 0.4**	**110.7 ± 0.4**
Normalized intensity	0.40	1.0	0.10	0.04	0.83
	0.47	**1.0**	**0.06**	**0.07**	**1.84**

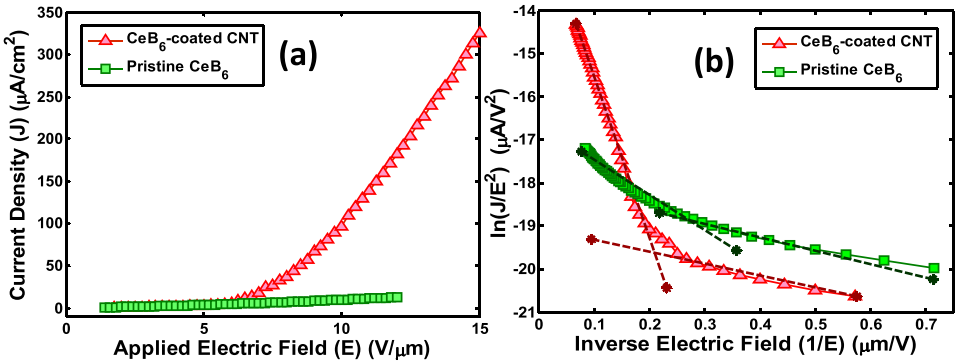

FIG. 4. (a) Average current density (J) versus applied electric field (E), (b) FN plot pristine CeB_6[12] and CeB_6-coated CNT films.

scattering process in MWCNT, the scenarios described above can explain the 2D band enhancement here observed.

The other possible reason for the 2D band enhancement is the healing effect of CeB_6 nanoparticles on CNTs. As demonstrated by Venezuela *et al.*[25] in graphene the area of the 2D peak and other two-phonon processes increases with a decrease in electronic linewidth or with increase in the electron lifetime due to a lower contribution from electron-phonon scattering and/or defect concentration. This is an indirect way in which defects can contribute to the intensity of the 2D band. This conclusion can be extrapolated to the CNTs[26] since the 2D band nature is the same for both cases. The intensity ratio I_D/I_G which is commonly used as the indication of defect concentration in CNTs is slightly increasing, implies a slight growth of defect density, while the D′ mode requiring defects for its activation decreases in area by almost four times, which again brings us to the opposite conclusion of a healing effect due to the CeB_6 coating[17] similar to the one reported for TiO_2 nanoparticles (NPs).[18] Following F. Inoue *et al.*,[18] we propose that the attachment of the CeB_6 nanoparticles to the CNT walls screens defects of the outer CNT shells from the Raman scattering process, assuming that the inner tubes have higher crystallinity than the outermost layers. It would also result in the increase of the sharpness of the Raman bands.

Since the same laser power was used in the spectra shown in Figure 3, the blue shift in the Raman spectra could be explained as a difference in sample temperature due to better thermal conductivity of the CeB_6-coated films.[27–30] This thermal effect would also contribute to the sharpness of the Raman bands (as represented by FWHM of the corresponding peak).[27] These results show that the chemical functionalization of CNTs by CeB_6 nanoparticles is clearly evidenced by Raman spectroscopy and in particular that the 2D band is highly sensitive to this functionalization.

The average current density (J) versus applied electric field (E) for pristine CeB_6 and for CeB_6-coated CNT are plotted and shown in Figure 4(a). The turn on field, i.e., the field required to achieve an emission current density of 10.0 $\mu A/cm^2$, was calculated from this graph and amounts to $E_{to}^{CeB_6} = (10.70 \pm 0.2)\,V/\mu m$ for pristine CeB_6[12] and $E_{to}^{CeB_6-CNT} = (6.35 \pm 0.2)\,V/\mu m$ for CeB_6-coated CNT. The threshold field (field required to achieve emission current density of 100.0 $\mu A/cm^2$), amounts to $E_{th}^{CeB_6-CNT} = (10.09 \pm 0.2)$ $V/\mu m$ for CeB_6-coated CNT. The threshold field for CeB_6 $E_{th}^{CeB_6}$ is not defined as it does not attend a maximum current density of 100.0 $\mu A/cm^2$ within the applied field limit.

The field enhancement factor of each sample was calculated from their respective FN plots as shown in Figure 4(b). The enhancement factor for the CeB_6-CNT composite is 4790 at the high field region which is 4.5 times of the maximum enhancement factor reported (1035) for CeB_6.[12]

Comparative results of maximum current density, turn-on field, threshold field, and enhancement factor for pure CeB_6,[12] and CeB_6-coated CNT films are given in Table II.

The fluctuation of the current density (cf) with respect to the mean value was calculated for CeB_6-coated CNT film at constant electric field using the formula

$$cf = \frac{|(x - \bar{x})|}{\bar{x}} \times 100\%, \tag{2}$$

where x is the maximum deviation from the mean value $\bar{x}$. The variation of current density with time in CeB_6-coated CNT is shown in Figure 5. The cf for CeB_6-coated CNT film was found to be ~3.0% at an electric field of 12.0 $V/\mu m$ with mean current density 182.17 $\mu A/cm^2$. The FE stability in CeB_6-coated CNT films decreased marginally compared to pristine CeB_6 ($cf \sim 1.5\%$).[12] Introduction of defects and increase of maximum current (15-fold) might have caused an increase in joule heating resulting into small increment in cf in the coated sample. But due to a greater dielectric constant of CeB_6 (with respect to air), the drifting distance of the electron decreases causing less joule heating for the coated sample.[31,32] These two combined effects lead to a small increment in

TABLE II. Turn-on field, threshold field, enhancement factor, and maximum current density for pristine CeB_6 nanorods,[12] and CeB_6-coated CNT films.

Sample	Turn-on field ($V/\mu m$) (@10 $\mu A/cm^2$)	Threshold field ($V/\mu m$) (@100 $\mu A/cm^2$)	Enhancement factor (high field region)	Maximum current density ($\mu A/cm^2$) (@12 $V/\mu m$)
Pristine CeB_6[12]	10.70 ± 0.2	…	1035	~12
CeB_6-coated CNT	6.35 ± 0.2	10.09 ± 0.2	4790	182.17

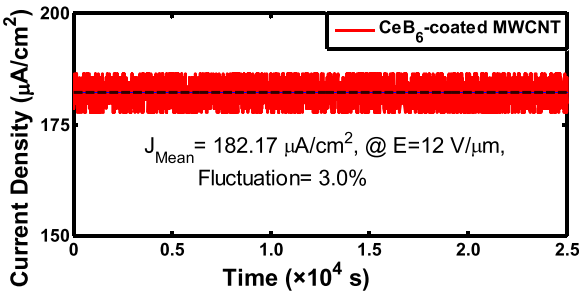

FIG. 5. FE current density versus time plots of CeB_6-coated CNT films, indicating significant improvement in temporal stability of the film.

current fluctuation in the coated sample. Also in case of coated CNT sample, the fluctuation contribution from both CNT and CeB_6 are added up to give the resulting total current fluctuation. Since the coated sample is less in quantity than CNT, so the fluctuation contribution from CNT will be more in total current contribution. As reported by Dean *et al.*,[33] the fluctuation in CNT increased roughly by an order of magnitude at room temperature (up to 225 °C named as peak fluctuation temperature). This emission current heated up the nanotubes which in turn increased the current fluctuation.[35]

The effective annulus (r_{eff}) of the emitter tip from which electron emission takes place can be calculated using the following equation,[34]

$$r_{eff} = \frac{me^{y_0/2}}{\sqrt{\pi}ab\varphi}, \tag{3}$$

where m is the slope and y_0 is the Y-axis intercept of the FN plot, φ is the work function of the material, a and b are the constants as given in Eq. (1). For the pristine CeB_6 film on Si,[12] the effective annulus comes out to be 0.056 nm in the high field region and 0.003 nm in the low field region, whereas for the CeB_6-coated CNT, it is 8.0 nm in the high field region (16 times more) and 0.034 nm in the low field region (10 times more). This is in accordance with the enhancement of β factor in the case of CeB_6-coated CNT film compared to pristine CeB_6. This fact, along with introduction of defects (as confirmed by Raman spectroscopy result) within CNT explains the significant rise (~16 times) in emission current density of the CeB_6-coated CNT films compared to that of pristine CeB_6. It is also observed that the structural stability of CeB_6-coated CNTs increases due to the CeB_6 coating (results not shown).

Comparing overall results of these films, it is clear that CeB_6-coated films have higher emission current, higher enhancement factor and lower turn-on and threshold fields than pristine CeB_6. The decrease in temporal stability is marginal. Therefore, CeB_6-coated CNT film comes up a better replacement for hexaborides as electron emitting material for applications like electron source in FE microscopes.

IV. CONCLUSION

A detailed FE analysis was carried out on CeB_6-coated CNT films grown by combining MPECVD and hydrothermal synthesis routes. Significant increment in the FE current density, stability and enhancement factor in CeB_6-coated CNT film with an appreciable decrement in turn on and threshold field as compared to pristine CeB_6[12] was observed. Chemical functionalization of CNT by CeB_6 nanoparticles was evident from Raman spectroscopy. The results are understood on the basis of (i) introduction of defects within CNT, (ii) increase in number of electron emission sites and (iii) increase in effective annulus. The improvement in FE properties in CeB_6-coated CNT indicates it is possible application as electron emitter for FE microscopes in future.

To the best of our knowledge, FE properties of CeB_6 coated CNT and its comparison with pristine CeB_6 is being reported for the first time which might lead to a new technology of electron source based device fabrication.

ACKNOWLEDGMENTS

R.P. thanks Professor V. D. Vankar, Professor P. Srivastava, and Ms. Debalaya Sarker (Department of Physics, IIT Delhi) for valuable discussions, IIT Delhi and DAAD for financial assistance. S.G. acknowledges partial financial support from CSIR, India. A.K.G. thanks DST, Government of India for financial assistance. H.S. acknowledges financial support from the Deutsche Forschungsgemeinschaft (DFG SCHM1663/4). E.S. acknowledges financial support from DFG research Project ZA146/22-1, and R.D.R. acknowledges DFG-Research Unit 1713 "SMINT."

[1]R. H. Fowler and L. Nordheim, Proc. R. Soc. London, Ser. A **119**, 173 (1928).
[2]R. G. Forbes, Nanotechnology **23**, 095706 (2012).
[3]Y. Saito and S. Uemura, Carbon **38**, 169 (2000).
[4]S. Motojima, Y. Takahashi, and K. Sugiyama, J. Cryst. Growth **44**, 106 (1978).
[5]Y. Zhao, L. Ouyang, C. Zou, J. Xu, Y. Dong, and Q. Fan, J. Rare Earths **28**, 424 (2010).
[6]H. Zhang, J. Tang, J. Yuan, J. Ma, N. Shinya, Nakajima K, H. Murakami, T. Ohkubo, and L. C. Qin, Nano Lett. **10**, 3539 (2010).
[7]W. Xiaoju, L. Zulun, Q. Kangcheng, C. Zexiang, W. Zhigang, and J. Yadong, J. Phys. D Appl. Phys. **40**, 4775 (2007).
[8]W. Wei, K. Jiang, Y. Wei, P. Liu, K. Liu, L. Zhang, Q. Li, and S. Fan, Appl. Phys. Lett. **89**, 203112 (2006).
[9]M. Jha, R. Patra, S. Ghosh, and A. K. Ganguli, RSC Adv. **2**, 7875 (2012).
[10]M. Kumari, S. Goutam, P. V. Shah, S. Pal, U. S. Ojha, and A. Kumar, Appl. Phys. Lett. **101**, 123116 (2012).
[11]M. Jha, R. Patra, S. Ghosh, and A. K. Ganguli, J. Solid State Chem. **194**, 173 (2012).
[12]M. Jha, R. Patra, S. Ghosh, and A. K. Ganguli, J. Mater. Chem. **22**, 6356 (2012).
[13]S. K. Srivastava, V. D. Vankar, and V. Kumar, Thin Solid Films **515**, 1552 (2006).
[14]R. Patra, S. Ghosh, H. Sharma, and V. D. Vankar, Adv. Mat. Lett. **4**, 849 (2013).
[15]R. D. Rodriguez, M. Toader, S. Hermann, E. Sheremet, S. Müller, and O. D. Gordan, Nanoscale Res. Lett. **7**, 682 (2012).
[16]M. Sveningsson, R. E. Morjan, O. A. Nerushev, Y. Sato, J. Bäckström, E. E. B. Campbell, D. Malsch, and J. A. Schaefer, Appl. Phys. A Mater. Sci. Process **73**, 409 (2001).
[17]A. C. Ferrari and D. M. Basko, Nat. Nanotechnol. **8**, 235 (2013).
[18]F. Inoue, R. A. Ando, and P. Corio, J. Raman Spectrosc. **42**, 1379 (2011).
[19]Y. Miyauchi, R. Saito, K. Sato, Y. Ohno, S. Iwasaki, T. Mizutani, J. Jiang, and S. Maruyama, Chem. Phys. Lett. **442**, 394 (2007).
[20]Y. Ohno, S. Iwasaki, Y. Murakami, S. Kishimoto, S. Maruyama, and T. Mizutani, Phys. Status Solidi B **244**, 4002 (2007).
[21]G. A. M. Sáfar, H. B. Ribeiro, L. M. Malard, F. O. Plentz, C. Fantini, A. P. Santos, and Y. M. Idemori, Chem. Phys. Lett. **462**, 109 (2008).

[22]G. A. M. Sáfar, H. B. Ribeiro, C. Fantini, F. O. Plentz, A. P. Santos, D. DeFreitas-Silva, and Y. M. Idemori, Carbon **48**, 377 (2010).
[23]G. A. M. Sáfar, A. Malachias, R. Magalhães-Paniago, M. V. Marinho, and H. O. Stumpf, J. Phys. Chem. C **116**, 25611 (2012).
[24]P. A. M. van der Heide, H. W. ten Cate, L. M. ten Dam, R. A. de Groot, and A. R. de Vroomen, J. Phys. F: Met. Phys. **16**, 1617 (1986).
[25]P. Venezuela, M. Lazzeri, and F. Mauri, Phys. Rev. B **84**, 035433 (2011).
[26]M. Dutta, V. Nicolosi, E. Obratzsova, A. A. Koós, A. Crossley, and N. Grobert, Mater. Express **1**, 201 (2011).
[27]A. Jorio *et al*., Phys. Rev. B **66**, 115411 (2002).
[28]H. D. Li *et al*., Appl. Phys. Lett. **76**, 2053 (2000).
[29]F. Huang, K. T. Yue, P. H. Tan, S. L. Zhang, S. Zujin, X. Zhou, and Z. Gu, J. Appl. Phys. **84**, 4022 (1998).
[30]P. V. Huong, R. Cavagnat, P. M. Ajayan, and O. Stephan, Phys. Rev. B **51**, 10048 (1995).
[31]V. K. Kayastha, B. Ulmen, and Y. K. Yap, Nanotechnology **18**, 035206 (2007).
[32]A. Pandey, A. Prasad, J. P. Moscatello, and Y. K. Yap, ACS Nano **4**, 6760 (2010).
[33]K. A. Dean, B. R. Chalamala, B. F. Coll, Y. Wei, C. G. Xie, and J. E. Jaskie, New Diamond Front. Carbon Technol. **12**, 165 (2002). Available at http://www.myu-inc.jp/myukk/NDFCT/archives/pdf/NDFCT394.pdf. See Ref. 35.
[34]A. Di Bartolomeo, A. Scarfato, F. Giubileo, F. Bobba, M. Biasiucci, and A. M. Cucolo, Carbon **45**, 2957 (2007).
[35]*Carbon Nanotube and Related Field Emitters: Fundamentals and Applications*, edited by Yahachi Saito (John Wiley & Sons, New York, 2010), p. 137.